Society For Biomaterials

Suppressing inflammation and enhancing osteogenesis using novel CS-EC@Ca microcapsules

Xiaoman Li,[1] Bing Han,[1] Xiaoyan Wang,[1] Xuejun Gao,[1] Fuxin Liang,[2] Xiaozhong Qu,[3] Zhenzhong Yang[2]

[1]Department of Cariology and Endodontology, Peking University School and Hospital of Stomatology, Beijing, 100081, China
[2]State Key Laboratory of Polymer Physics and Chemistry, Institute of Chemistry, Chinese Academy of Sciences, Beijing, 100190, China
[3]College of Materials Science and Opto-Electronic Technology, University of Chinese Academy of Sciences, Beijing, 100049, China

Received 12 April 2018; revised 9 July 2018; accepted 25 July 2018
Published online 5 October 2018 in Wiley Online Library (wileyonlinelibrary.com). DOI: 10.1002/jbm.a.36517

Abstract: The aim of this study was to investigate the suppression of inflammation and enhancement of osteogenesis using chitosan-coated calcium hydroxide-loaded microcapsules (CS-EC@Ca microcapsules) *in vivo*. Circular defects were created in the mandibular bones of rabbits and filled with $Ca(OH)_2$, Bio-oss, or CS-EC@Ca microcapsules, and rabbits without drug implantation served as the controls. Lipopolysaccharides were injected *in situ* daily in all groups for 7 days. Mandibular bones were investigated at 4 and 12 weeks after surgery using micro-CT, histological observations, and real-time PCR analysis. At the postoperation, there was more substantial nascent bone in the microcapsule and Bio-oss groups than in the control group. The recovery of the rabbits in the $Ca(OH)_2$ group was slower than the control group, as determined using micro-CT and histological staining. Osteocalcin and collagen type I production was not significantly different between the microcapsule and Bio-oss groups ($p > 0.05$), but the expression levels of the two molecules were significantly increased compared to the control and $Ca(OH)_2$ groups at postoperation ($p < 0.05$). The mRNA transcript levels of inflammatory factors in the microcapsule group had the most reduced expression of IL-6 and TNF-α ($p < 0.05$). The microcapsules significantly reduced inflammation and promoted osteogenesis in this rabbit model of inflammatory bone destruction. Our findings indicate that CS-EC@Ca microcapsules hold potential for use in apical periodontitis treatment. © 2018 Wiley Periodicals, Inc. J Biomed Mater Res Part A: 106A: 3222–3230, 2018.

Key Words: apical periodontitis, osteogenesis, calcium hydroxide, microcapsules

How to cite this article: Li X, Han B, Wang X, Gao X, Liang F, Qu X, Yang Z. 2018. Suppressing inflammation and enhancing osteogenesis using novel CS-EC@Ca microcapsules. J Biomed Mater Res Part A 2018:106A:3222–3230.

INTRODUCTION

Oral infections, particularly apical periodontitis (AP) and periapical periodontitis, can lead to alveolar bone resorption around the root apex and tooth loss.[1,2] In the clinic, root canal therapy can remove microbiota from the root canal and thus promote alveolar bone repair.[3] The healing of alveolar bone depends on controlled infections and host factors.[4] In general, inflammation can be reduced and new bone can be formed in periapical bone defects merely due to the host's abundant blood supply and nonspecific immune system.[5] However, the healing process is long, taking approximately 6 months or even longer. Bone formation may require additional time due to low-level regeneration activity of the host, which depends on age, degree of infection, and general condition.[6]

In noninfectious bone defects, such as bone fractures, the healing process mainly relies on osteoblast differentiation and bone regeneration.[7] The difference between the management of infectious and noninfectious bone defects is the control of infection.[8,9] Therefore, the local dosage of preparations that suppress inflammation and enhance osteogenesis may benefit the repair of AP with large sized bone defects.

Calcium hydroxide ($Ca(OH)_2$) has long been used to treat pulpitis and periapical diseases as it can disinfect the infected root canal, dissolve necrotic tissue, and promote hard tissue formation.[10] The pure powder of $Ca(OH)_2$, however, can show high cytotoxic effects on adjacent tissues because of the strong alkaline environment created by its burst release.[11] To achieve an ideal $Ca(OH)_2$ endodontic application, ethyl cellulose (EC)-encapsulated $Ca(OH)_2$ microcapsules (EC@Ca microcapsules) were developed,[12] and it was shown that they have prolonged antibacterial activity, enhanced osteogenic properties, and reduced

Correspondence to: Xiaoyan Wang; e-mail: wangxiaoyan@pkuss.bjmu.edu.cn
Contract grant sponsor: the Natural Science Foundation of China; contract grant number: 51103001

cytotoxicity.[13] In addition, to avoid the burst release from EC@Ca microcapsules during the very early stage in neutral media, we previously also developed chitosan (CS)-coated EC@Ca microcapsules (CS-EC@Ca microcapsules).[14] CS-EC@Ca microcapsules showed pH-triggered release properties and improved antibacterial and osteogenic activities because of the characteristics of CS and their core–shell structure.[14]

Based on the promising results obtained *in vitro*, in the present study, we evaluated the osteogenic performance of CS-EC@Ca microcapsules *in vivo.* In the preliminary experiment, a rabbit model of AP using New Zealand white rabbits was established with a mandible bone defect and local LPS injection for 7 days. We hypothesized that the CS-EC@Ca microcapsules suppress inflammation and promote osteogenesis in this inflammatory bone destruction model. Our findings reveal that CS-EC@Ca microcapsules have great potential for use in AP treatment in the future.

MATERIALS AND METHODS

Preparation of CS-EC@Ca microcapsules

The CS-EC@Ca microcapsules were fabricated as described previously[14] with accurate adjustment of the pH of the solution system. The morphology and composition, particle size distribution, drug loading, and encapsulation efficiency of the microcapsules were characterized in the previous study. In addition to the sustained release of $Ca(OH)_2$, the CS-EC@Ca microcapsules also display pH-triggered release. *In vitro*, the CS-EC@Ca microcapsules exhibited prolonged antibacterial activity, remarkably reduced inflammation, and promoted osteogenesis with reduced cytotoxicity.[14] Figure 1 (A,B) show the schematic illustration of the preparation of the CS-EC@Ca microcapsules and their morphology, multilayer structure, and size distribution.[14]

Animals

Twenty-four healthy New Zealand white rabbits (approximately 3.0 kg in weight) were used in this study. For all rabbits, circular defects 8 mm in diameter were made in the two sides of the mandible body with no obvious effects on the eating habits of the rabbits.[15,16] The defects were assigned to 4 groups randomly as follows: group 1, defects were left untreated and these animals were used as blank controls (Control group); group 2, defects were filled with Bio-oss (particle size 0.25 mm–1 mm), which is a commercially available product consisting of devitalized bovine bone granules and spongy-like collagen (Geistlich, Wolhusen, Switzerland) (Bio-oss group); group 3, defects were filled with pure $Ca(OH)_2$ powder (Ca group); and group 4, defects filled with CS-EC@Ca microcapsules (microcapsule group). Peking University guidelines for the care and use of laboratory animals (No LA2016022) were observed. The animals were maintained on a normal, solid lab diet with access to regular tap water.

Surgical procedures

All operations were performed by one professional surgeon, as shown in Figure 2. The rabbits were anesthetized with 2% (w/v) pentobarbital sodium. After shaving the skin and disinfecting the surgical site, a parallel skin incision was made along the inferior border of the mandible on both sides, the muscle was detached, and the mandibular body was exposed. Under continuous saline irrigation, a rotating trephine burr was used to create circular defects with 8 mm diameter in the mandibular body, which was the critical size of the bone defects in rabbits.[17] Next, 0.2 g of Bio-oss, pure $Ca(OH)_2$ powder, or CS-EC@Ca microcapsules was implanted into the defects, and no implanted material was placed into the control group. The mucoperiosteal flaps and skin were carefully sutured over the defect area, and a 3-day course of penicillin (10^5 IU/kg of rabbits weight), was administered by intramuscular injection after the operations.

After the surgery, each rabbit received an injection of 1 mL LPS (50 μg/mL, L4391; Sigma, St. Louis, MO) into the bone defects every day for 7 days.[10] All animals in each group were maintained in their normal cages without any limitation and sacrificed by lethal intravenous administration of sodium pentobarbital at 4 and 12 weeks after surgery. Half the obtained mandibles were trimmed and fixed in 10% paraformaldehyde for micro-CT evaluation and histological observation, and the remaining mandibles were trimmed and placed into a liquid nitrogen container for gene expression analysis.

Microcomputed tomography (micro-CT) evaluation

After 48 h of fixing, high-resolution images of the fixed specimens were obtained using a micro-CT scanner (Inveon MM CT, SIEMENS, Munich, Germany) at 80 kV (X-ray source voltage), 500 μA (beam current), 1500 ms (exposure time), 9.08 μm (effective pixel size), and 360° (rotation angle). The obtained data were reconstructed from the volume of interest using COBRA (Exxim Computing Corporation, Pleasanton, CA) and scanning software (Inveon Acquisition Workplace, SIEMENS, Munich, Germany). After 3D reconstruction, the percentage bone volume (BV/TV) and bone mineral density (BMD) were calibrated and determined using Inveon Research Workplace.

Histological analysis

After micro-CT analysis, the specimens were fixed for another 4 days and then demineralized in 10% EDTA for 12 weeks at 37°C with a solution change every 2 days. Subsequently, the specimens were embedded in paraffin and sectioned (4 μm thickness) for staining.

Hematoxylin/eosin (HE) staining and Masson's trichrome staining were performed separately on the tissue slices according to the manufacturer's protocols, and the images were captured using light microscopy (CX21, Olympus, Japan) to evaluate the degree of osteogenesis and degradation of the implanted materials. Further quantitative histomorphometric evaluation was performed using BIOQUANT Software (Nashville, TN).[18] After scanning the Masson-stained sections using a biological microscope (Eclipse 80i, Nikon, Japan) and stitching the images together, the new bone formation, including adipose tissue volume/tissue volume (Ad.V/TV), bone volume/tissue volume (BV/TV), trabecular diameter (Tb.Dm),

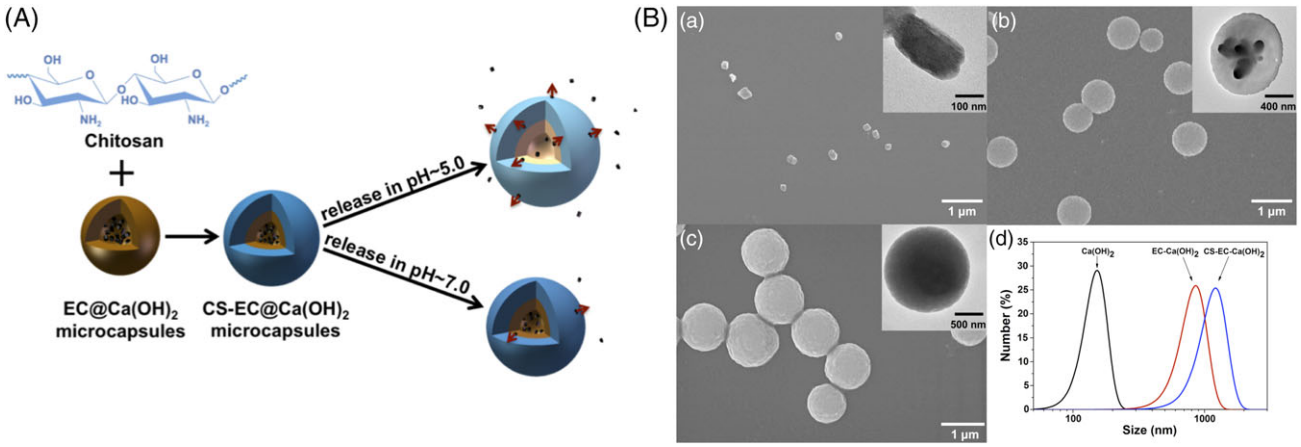

FIGURE 1. Schematic illustration and characterization of CS-EC@Ca microcapsules. (A) Schematic diagram of the preparation of CS-EC@Ca microcapsules. (B) Scanning electron microscopy images and transmission electron microscopy (inset) images of pure $Ca(OH)_2$ powder (a), EC@Ca microcapsules (b), and CS-EC@Ca microcapsules (c). Particle size distributions of $Ca(OH)_2$ and the microcapsules (d).

and trabecular number (Tb.N), was assessed quantitatively. These parameters were then evaluated in a blinded manner by an independent investigator.

Immunohistochemistry

For immunohistochemistry, the tissue slices were deparaffinized and rehydrated. Then, they were treated with 3% hydrogen peroxide for 20 min to inactivate endogenous peroxidase. Next, they were processed using phosphate buffer solution (PBS) for 30 min to block unspecific ligations. Following thorough washing, primary antibodies that were diluted 1:200, including osteocalcin (OCN) antibody (mouse monoclonal, ab13420; Abcam, Cambridge, United Kingdom) and collagen type I (COL I) antibody (mouse monoclonal, GTX26308, GeneTex, CA), were applied at 4°C overnight, and then the slices were washed and stained with HRP-conjugated secondary antibody according to the manufacturer's protocol (PV-9000; ZSGB-BIO, Beijing, China). Finally, a diaminobenzidine (DAB, ZSGB-BIO) kit was used for color development and was followed by hematoxylin counterstaining. The slices were then examined under a light microscope (CX21, Olympus).

Quantitative real-time polymerase chain reaction (PCR)

Under liquid nitrogen, the flash-frozen specimens were ground into a powder. The RNA was then extracted using TRIzol (Invitrogen, Carlsbad, CA) and converted into cDNA using the RevertAid First Strand cDNA Synthesis Kit (Thermo Scientific, Waltham, MA) according to the manufacturer's instructions. Quantitative real-time PCR was performed using the SYBR Green Kit (Roche, USA) on an ABI PRISM 7500 Real-Time PCR machine (Applied Biosystems, Foster City, CA). The primers (5′–3 ′) for OCN, COL I, interleukin (IL)-6, and tumor necrosis factor (TNF)-α are listed in Table I. The data were analyzed using the comparative CT ($2^{-\triangle\triangle CT}$) method.

Statistical analysis

All measurements were carried out in triplicate, and quantitative data were expressed as the mean ± standard deviation. All data were statistically analyzed by one-way analysis of variance, followed by Tukey's *post hoc* test. A value of $p < 0.05$ was considered statistically significant.

RESULTS

Gross morphology and micro-CT observation

After both 4 and 12 weeks in the control group, gross morphological observation revealed that the defects exhibited no obvious signs of recovery and remained as conspicuous defects with filled fibrous tissues [Fig. 3(A)]. The mandible defects remained in the unrepaired area and necrotic bone was observed in the surrounding tissues after 4 and 12 weeks in the Ca group [marked with red arrows in Fig. 3 (A,C,G)]. The 3D reconstruction of the micro-CT images also revealed that the control group and Ca groups showed similar BMD and BV/TV values [Fig. 3(B,C)]. However, the regenerated bone tissue was flush with the surrounding host bone tissue in the CS-EC@Ca microcapsule group after 4 weeks, which was similar to that observed in the Bio-oss group. After 12 weeks, defects in the CS-EC@Ca microcapsule and Bio-oss groups healed well, and the new bone was indistinguishable from the host bone. Micro-CT results also showed substantial nascent bone formation in the microcapsule and Bio-oss groups at 12 weeks post-implantation.

To quantify the calcification of the newly formed bone in the repaired mandibles in the different groups, local BMD and the BV/TV ratio were assessed by micro-CT analysis at 4 and 12 weeks postsurgery. As shown in Figure 3(B), the microcapsule group showed a relatively higher BMD than the control and Ca groups ($p < 0.05$), and the results observed in the microcapsule group were not significantly different from those in the Bio-oss group ($p > 0.05$). The results also indicated that the BV/TV ratio closely corresponded with the BMD values for each group [Fig. 3(C)].

Histological assessment

As shown in Figure 4(A), the boundary between the defect area and the host bone tissue was clearly identified in all the groups at 4 weeks post-implantation. In the control and Ca

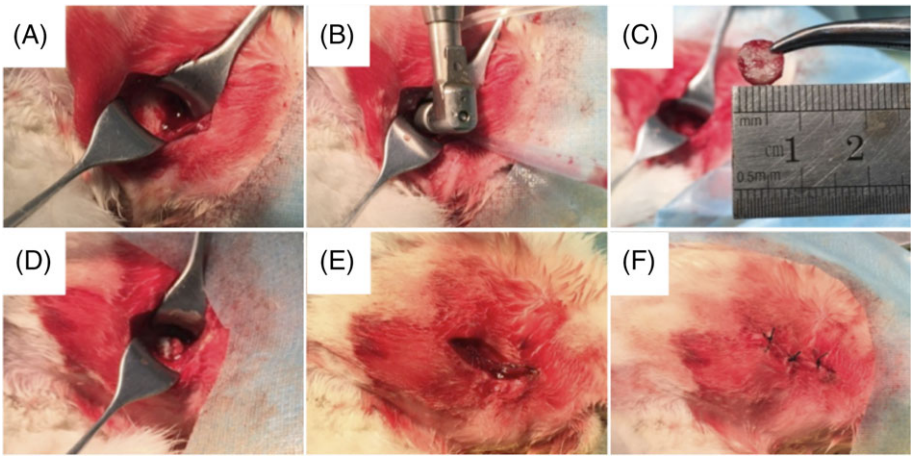

FIGURE 2. Establishment of bone defects in the rabbits. (A) Mandibular bone exposure; (B) circular critical-sized defect creation; (C) sclerite removal; (D) material implantation; (E) mucoperiosteal flap suture; (f) skin suture.

groups, there were numerous fat vacuoles in the defect area with little fibrous tissue or new bone. In particular, more blank areas were found in the Ca group than in the control group. In contrast, HE staining revealed fibrous connective tissue around the implanted material in both the Bio-oss and microcapsule groups. Masson staining showed that the fibrous tissue was mainly composed of newly formed collagen fibers, which were stained green. The filled materials of both the Bio-oss and microcapsule groups were observed in the border and center of the defects and were surrounded with fibrous tissue and some newly regenerated bone.

At 12 weeks post-implantation, the interface between the nascent bone and the host bone remained distinguishable in the control and Ca groups. There were fewer trabeculae and the mature bone marrow cavities had only a thin layer of lamellar trabeculae in the defect sites of both groups. In the Ca group, the center defect exhibited no obvious recovery but was filled with abundant fibrous tissue and some immature bone. However, in the Bio-oss and microcapsule groups, the interface was indistinguishable because mature bone structures filled the bone defect region in both groups. Moreover, both groups showed normal and regular bony trabeculae and mature bone marrow cavities. Masson staining revealed that the original green-stained collagen fibers were replaced by mature woven bone in the central bone defect region in these groups. However, in the Bio-oss group, the implanted materials were not replaced and were surrounded by less osteoid. In the microcapsule group, most of the implanted material was replaced, the defect was almost fully covered by mature lamellar bone, and the ossein in green was spread out consistently in the new bone matrix.

BIOQUANT Software was used to quantitatively calculate the amount of newly formed bone after implantation [Fig. 4 (B)]. The ratios of Ad.V/TV in the control and Ca groups were significantly higher than those in the Bio-oss and microcapsule groups after 4 and 12 weeks of implantation ($p < 0.05$). The BV/TV ratio in the microcapsule group was higher than in the Bio-oss group after 12 weeks of implantation, while that in the Bio-oss group was significantly higher than the ratios in the other two groups after 12 weeks of implantation ($p < 0.05$). There was no significant difference in Tb.Dm values between the groups ($p > 0.05$). The Tb.N. value in the microcapsule group was higher than in the Bio-oss group after 12 weeks of implantation, while that in the Bio-oss group was significantly higher than the values in the other two groups after 12 weeks of implantation ($p < 0.05$).

OCN and COL I production in the bone defects

OCN, a marker of bone maturation, was prevalent within the defects in all implantation groups. Notably, the most intense staining was observed in the microcapsule and Bio-oss groups at 4 and 12 weeks post-implantation compared with the control group [Fig. 5(A)]. The mRNA expression levels of OCN [Fig. 5(C)] in the microcapsule and Bio-oss groups were similar after 4 and 12 weeks of implantation ($p > 0.05$). Moreover, the expression levels in the Bio-oss and microcapsule groups were significantly higher than the control group at 4 weeks ($p < 0.05$). At 12 weeks, the expression levels in the microcapsule group was significantly higher than the control and Ca groups at the same time point ($p < 0.05$).

The expression of COL I, which is a key component as a scaffold and template for mineral formation, was significantly increased in the microcapsule group compared to the control group ($p < 0.05$), but the expression was not obviously different compared to the Bio-oss group at 4 and 12 weeks after implantation ($p > 0.05$) [Fig. 5(B,D)].

Inflammatory gene expression

The mRNA transcript levels of inflammatory factors (IL-6 and TNF-α) are shown in Figure 6. The microcapsule group displayed the most reduced expression of IL-6 and TNF-α ($p < 0.05$). The differences between the control and Bio-oss group were not significant ($p > 0.05$), but the expression levels were significantly higher than the Ca group at both 4 and 12 weeks post-implantation ($p < 0.05$).

DISCUSSION

In a previous study, CS-EC@Ca microcapsules were confirmed to be core-shell structures with a pH-triggered

TABLE I. Primer Sequences (5′–3′) for Quantitative Real-Time PCR

Name	Forward Primer	Reverse Primer
GAPDH	CTGATGCCTCCATGTTTGTG	GGATGCAGGGATGATGTTCT
OCN	GAAGCCCAGCGGTGCA	CACTACCTCGCTGCCCTCC
COL I	AGCGTGGCCTACCTGGATGAAGC	ATGGGCGCGATGTCGGTGATGG
IL-6	GCTTGAGGGTGGCTTCTTC	GCTTGAGGGTGGCTTCTTC
TNF-α	TCCGTGAAAACAGAGCAGAA	GAGCAGAGGTTCGGTGATGT

control release property.[14] The microcapsules exhibited prolonged antibacterial activity against refractory strains of *Enterococcus faecalis in vitro.* Additionally, the CS-EC@Ca microcapsules reduced inflammation and promoted osteogenesis, which can be beneficial for the healing of bone defects in AP cases.[14] In this study, we focused on the biological effects of CS-EC@Ca microcapsules using a rabbit model of AP.

The molar teeth of mice or rats were used to investigate the pathogenesis or molecular mechanisms of AP.[19] However, the periapical lesion size in mouse/rat molars is difficult to standardize; therefore, these models can seldom be used to evaluate the prognosis of AP. LPS was recognized as an initiation factor for a series of inflammatory and immune responses in periapical lesions.[20,21] LPS generated by Gram-negative bacteria infiltrating the root canal and periapical tissues can induce the expression of many types of inflammatory cytokines, such as TNF and IL-6, which were reported to participate in alveolar bone resorption, as well as promote the survival and differentiation of preosteoclasts.[22] Therefore, LPS has been used as a stimulus for creating an inflammatory environment *in vitro* and *in vivo.*[2,21] LPS injection causes extensive loss of mouse calvaria.[10] However, bone healing may be different between the calvaria and mandibular bone. In general, the rabbit mandibular bone has been used to evaluate the osteogenic effects of drugs or materials in stomatology.[16] In our preliminary experiment, critical-sized mandibular bone defects (8 mm in diameter) were created in a rabbit model with an LPS-induced inflammatory microenvironment to simulate AP. The results of the preliminary experiment indicated that LPS prolonged the duration of bone defect healing. We found that the control group with LPS stimulation showed little regenerated new bone, but fibrous tissue filled in the defect sites at 12 weeks

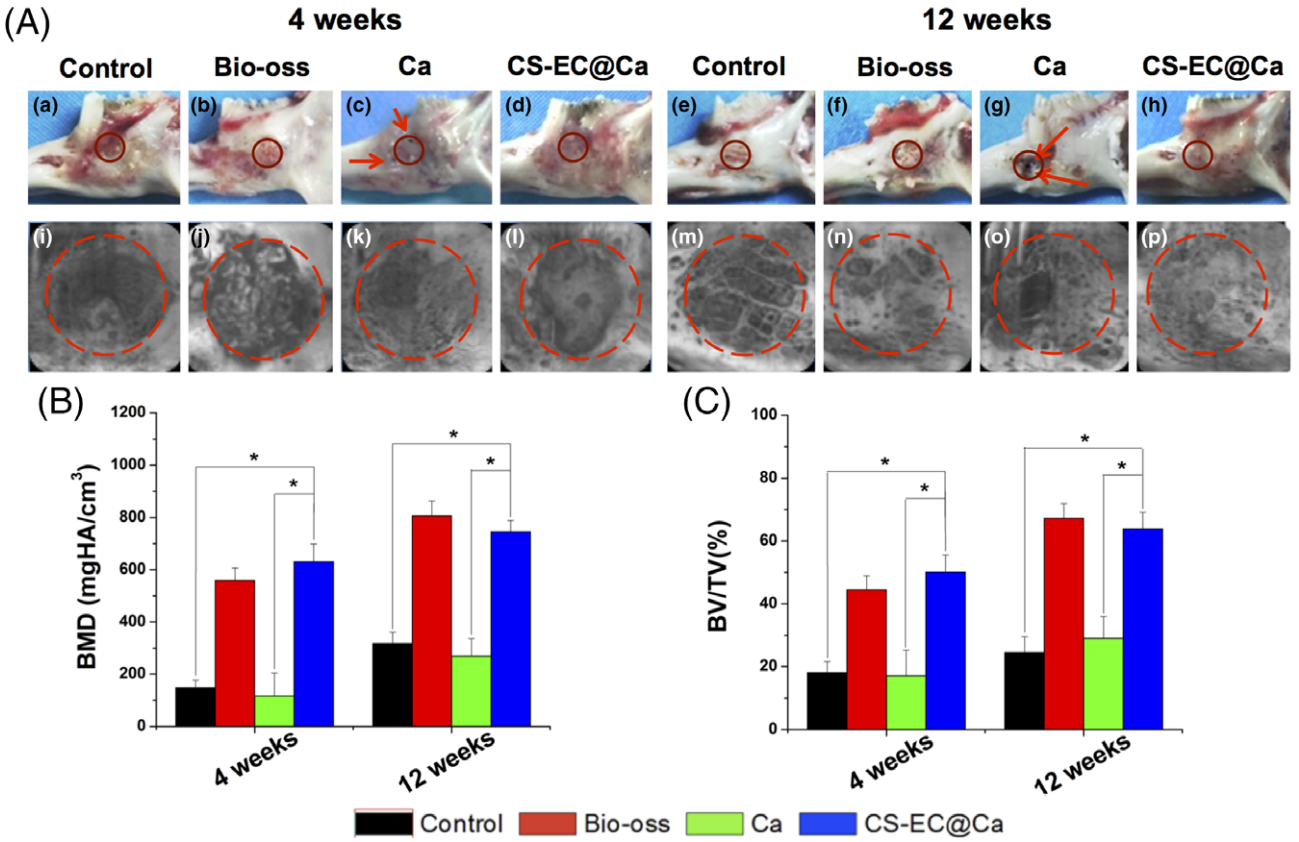

FIGURE 3. Gross photos and representative 3D micro-CT images of rabbit mandibular bone defect repair (A) and quantitative analysis of bone mineral density (BMD) (B) and the ratio of the bone volume/total volume (BV/TV) (C) at 4 and 12 weeks after implantation.

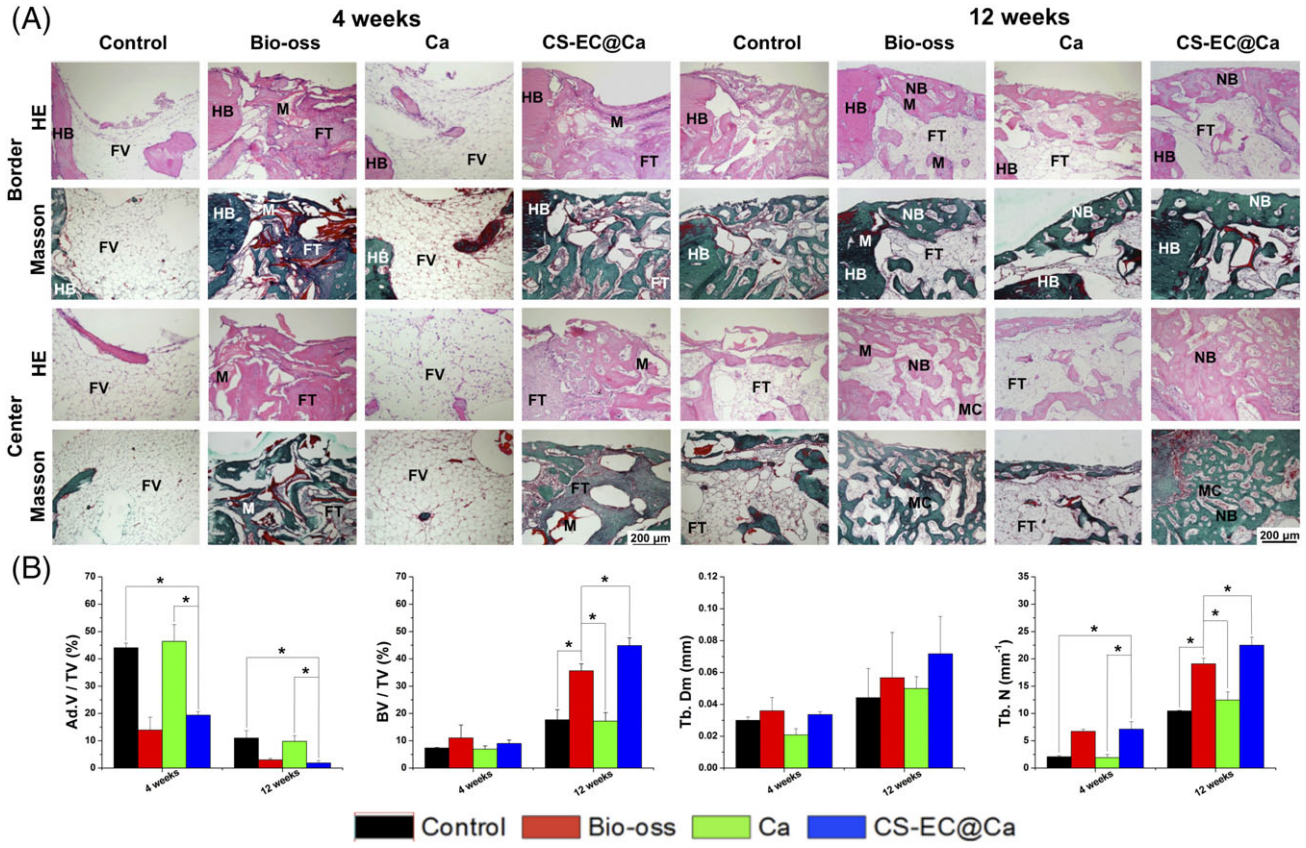

FIGURE 4. Histological analysis of bone formation at 4 and 12 weeks after implantation. (A) H&E staining and Masson's trichrome staining. (B) Quantitative analysis using BIOQUANT software. (M: material; HB: host bone; NB: nascent bone; MC: medullary cavity; FV: fat vacuoles; FT: fibrous tissue).

postsurgery; however, the same bone defects without LPS revealed more new bone in the edge of the defects, which is consistent with a previous report.[15]

$Ca(OH)_2$ is widely used for root canal treatments because of its antibacterial, anti-inflammatory, and osteogenic activities.[11] In our study, the expression of inflammatory factors in the Ca group was significantly lower than the control group, which indicated that $Ca(OH)_2$ exerted an anti-inflammatory effect in the LPS-mediated inflammation environment. This effect is likely because $Ca(OH)_2$ hydrolyzed lipid A to destroy the structure and attenuate the toxicity of LPS.[10] However, there was less nascent bone in the Ca group than the Bio-oss and microcapsule groups, which is consistent with the finding that pure $Ca(OH)_2$ powder is associated with a burst release in a strong local alkaline environment, which inhibits bone formation.

Bio-oss is a commercially available bone substitute used for dental applications in both research and in clinical settings.[23] However, controversial ethical issues of animal welfare, time-consuming manufacturing process and high price are likely to impede the clinical application of Bio-oss.[24] In this study, the expression of inflammatory factors was significantly higher in the Bio-oss group than in the Ca and microcapsule groups in the simulated environment for 12 weeks after surgery, which may be adverse to controlling inflammation in AP cases. However, the Bio-oss group showed more new bone than the control group in our study due to its special structure and ion release properties. As an osteoconductive material, Bio-oss consists of devitalized bovine bone granules and spongy-like collagen.[25] Relevant research indicates that the surface of Bio-oss can promote cell adhesion and bone deposition; moreover, the release of Ca^{2+} from Bio-oss has also been reported to be theoretically beneficial to osteogenesis.[25] Although there were no obvious anti-inflammatory effects observed with Bio-oss, these data indicate that Bio-oss can promote bone regeneration. Additional studies of the interaction of Bio-oss, inflammatory factors, and bone formation are needed.

In the microcapsule group, the anti-inflammatory effects were similar to those observed in the Ca group. Moreover, bone regeneration in the CS-EC@Ca microcapsule group was obviously promoted compared to the Ca group, which was similar to the Bio-oss group. This microcapsule system can rapidly release $Ca(OH)_2$ in acidic inflammatory microenvironments to increase the pH.[14] Such a system would inactivate LPS and thus prevent it from inhibiting inflammation while preventing bone resorption. When the microenvironment becomes neutral or slightly alkaline because of $Ca(OH)_2$, the

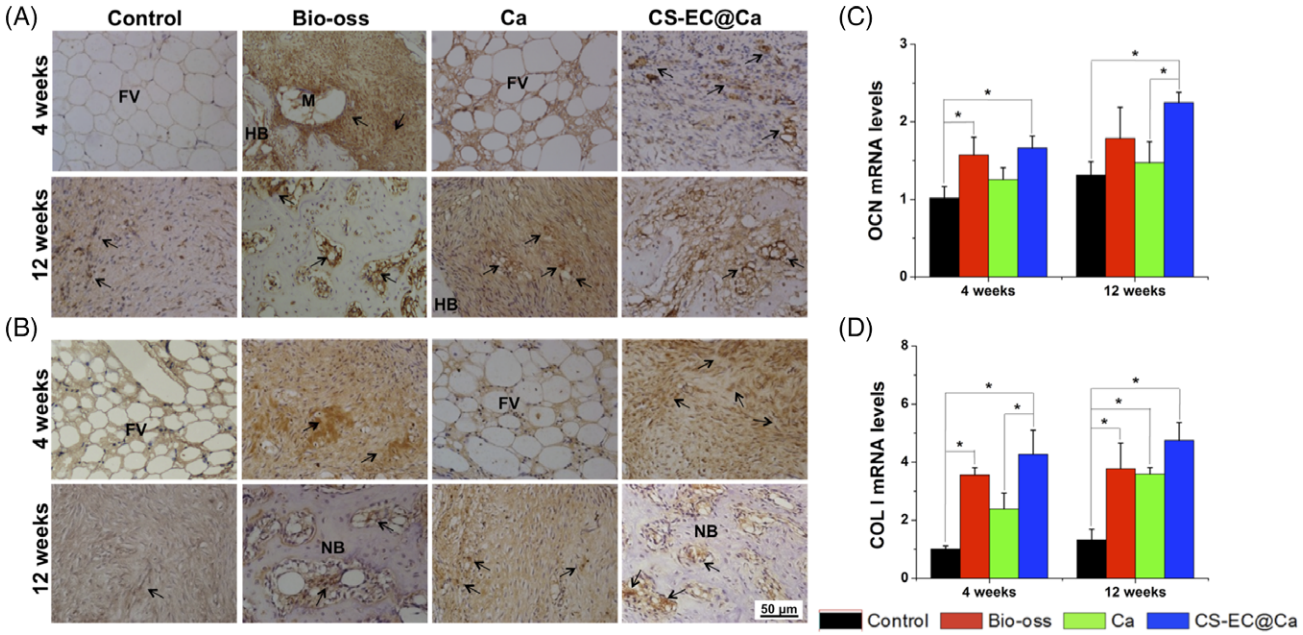

FIGURE 5. OCN and COL I production in rabbit mandibular bone defects. Immunohistological staining of OCN (A) and COL I (B). The mRNA transcript levels of OCN (C) and COL I (D). Arrows denote the positive expression of OCN and COL I.

release of $Ca(OH)_2$ decreases in response. Lasting low-dose release can maintain an alkaline environment and is beneficial for osteogenesis. The dissociation of a suitable concentration of Ca^{2+} was found to be critical for promoting osteoblast viability and bone mineralization.[26] Although OH^- does not affect bone mineralization directly, it is important to adjust the extracellular pH to maintain a balance between bone formation and resorption. Therefore, a slightly alkaline microenvironment (pH 8.0–8.5) is beneficial for inducing osteogenesis.[12,27] Thus, CS-EC@Ca microcapsules not only have anti-inflammatory effects but also promote bone regeneration in an AP environment.

However, equally important is the stable degradation of the implanted microcapsules, which could be beneficial for bone forming. CS and EC, as the shell material of microcapsules, are not cytotoxic and degradable and can therefore promote cell proliferation.[28,29] The main histological findings in our study revealed significant degradation of the microcapsules, especially in the period from 4 to 12 weeks, whereas the Bio-oss was only slightly degraded at 4 weeks after surgery and showed no obvious further degradation at 12 weeks after surgery, which is consistent with previous reports.[30] Moreover, the drug release from the CS-EC@Ca microcapsules is steady and sustained for osteogenesis, and with inner drug release, a perforated channel structure is formed, which is conducive to cell adhesion and proliferation.[14] Bio-Oss, on the other hand, degrades slowly and remains even 11 years after implantation, which hampers further bone formation and full regeneration in those areas.[31,32] During the production process, organic parts are

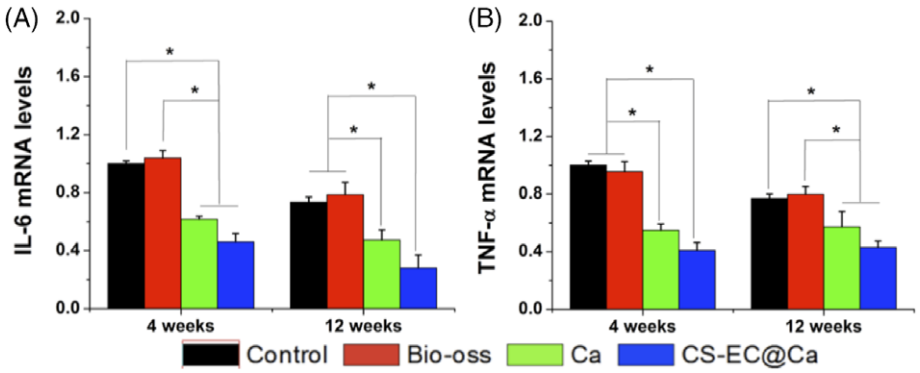

FIGURE 6. The mRNA expression levels of IL-6 (A) and TNF-α (B) at bone defect sites at 4 and 12 weeks post-implantation.

removed from bovine bone and the remaining Ca-containing bone structures are processed to slowly degradable granules.[33] This may be interpreted as a wound healing process with incorporation of a body foreign material rather than bone regeneration.[34]

However, there are several limitations to our research. The anti-inflammatory activity of CS-EC@Ca microcapsules was shown on the mRNA level, and this study was preliminary. Of equal importance for an anti-inflammatory study is the protein level of these molecules. In future research, it must be verified whether microcapsules have anti-inflammatory effects at the protein level.

CONCLUSIONS

In summary, this study showed the osteogenic performance of CS-EC@Ca microcapsules in a rabbit model of AP compared to Bio-oss and pure $Ca(OH)_2$ powder. *In vivo*, the results of micro-CT analysis, histological analysis, and mRNA expression analysis confirmed that microcapsules significantly reduced inflammation and promoted osteogenesis in an inflammatory environment. A follow-up study of the anti-inflammatory effects of microcapsules on the protein level, as well as mechanical performance testing, such as for the strength and elasticity of the restored bone, should be performed in the future with more specimens per group. Nevertheless, our findings indicate that CS-EC@Ca microcapsules improve the innate properties of $Ca(OH)_2$ and, therefore, hold potential for use in AP treatment.

ACKNOWLEDGMENTS

Thanks to Chengfei Zhang from the University of Hong Kong for guidance with this article.

REFERENCES

1. Zhang R, Huang S, Wang L, Peng B. Histochemical localization of Dickkopf-1 in induced rat periapical lesions. J Endod 2014;40:1394–1399.
2. Suzuki N, Takimoto K, Kawashima N. Cathepsin K inhibitor regulates inflammation and bone destruction in experimentally induced rat periapical lesions. J Endod 2015;41:1474–1479.
3. Yu VS, Khin LW, Hsu CS, Yee R, Messer HH. Risk score algorithm for treatment of persistent apical periodontitis. J Dent Res 2014;93:1076–1082.
4. Cotti E, Schirru E, Acquas E, Usai P. An overview on biologic medications and their possible role in apical periodontitis. J Endod 2014;40:1902–1911.
5. Al-Ahmad A, Ameen H, Pelz K, Karygianni L, Wittmer A, Anderson AC, Spitzmuller B, Hellwig E. Antibiotic resistance and capacity for biofilm formation of different bacteria isolated from endodontic infections associated with root-filled teeth. J Endod 2014;40:223–230.
6. Yu VS, Messer HH, Shen L, Yee R, Hsu CS. Lesion progression in post-treatment persistent endodontic lesions. J Endod 2012;38:1316–1321.
7. Lee SJ, Park YJ, Park SN, Lee YM, Seol YJ, Ku Y, Chung CP. Molded porous poly (L-lactide) membranes for guided bone regeneration with enhanced effects by controlled growth factor release. J Biomed Mater Res A 2001;55:295–303.
8. Ling E, Ling LF, Liu HC, Wang DS, Shi ZP, Wang JC, Luo W, Lv Y. The effect of calcium phosphate composite scaffolds on the osteogenic differentiation of rabbit dental pulp stem cells. J Biomed Mater Res A 2015;103:1732–1745.
9. Zhao NB, Wang X, Qin L, Zhai M, Yuan J, Chen J, Li DH. Effect of hyaluronic acid in bone formation and its applications in dentistry. J Biomed Mater Res A 2016;104:1560–1569.
10. Guo J, Yang D, Okamura H, Teramachi J, Ochiai K, Qiu L, Haneji T. Calcium hydroxide suppresses *Porphyromonas endodontalis* lipopolysaccharide-induced bone destruction. J Dent Res 2014;93:508–513.
11. Narita H, Itoh S, Imazato S, Yoshitake S, Ebisu S. An explanation of the mineralization mechanism in osteoblasts induced by calcium hydroxide. Acta Biomater 2010;6:586–590.
12. Nuria MC, Margarita B, Sivan S, Hayward A, Stanley J, Parry NM, Edelman ER, Artzi N. Regulation of dendrimer/dextran material performance by altered tissue microenvironment in inflammation and neoplasia. Sci Transl Med 2015;7:272ra211.
13. Han B, Wang XY, Liu JG, Liang FX, Qu XZ, Yang ZZ, Gao XJ. The biological performance of calcium hydroxide-loaded microcapsules. J Endod 2013;39:1030–1034.
14. Li XM, Han B, Wang XY, Gao XJ, Liang FX, Qu XZ, Yang ZZ. Chitosan-decorated calcium hydroxide microcapsules with pH-triggered release for endodontic applications. J Mater Chem B 2015;3:8884–8891.
15. Zhang X, Xu M, Song L, Wei Y, Lin Y, Liu W, Heng BC, Peng H, Wang Y, Deng X. Effects of compatibility of deproteinized antler cancellous bone with various bioactive factors on their osteogenic potential. Biomaterials 2013;34:9103–9114.
16. Zhang X, Cai Q, Liu H, Heng BC, Peng H, Song Y, Yang Z, Deng X. Osteoconductive effectiveness of bone graft derived from antler cancellous bone: An experimental study in the rabbit mandible defect model. Int J Oral Max Surg 2012;41:1330–1337.
17. Peric M, Dumic-Cule I, Grcevic D, Matijasic M, Verbanac D, Paul R, Grgurevic L, Trkulja V, Bagi CM, Vukicevic S. The rational use of animal models in the evaluation of novel bone regenerative therapies. Bone 2015;70:73–86.
18. Scimeca M, Feola M, Romano L, Rao C, Gasbarra E, Bonanno E, Brandi ML, Tarantino U. Heavy metals accumulation affects bone microarchitecture in osteoporotic patients. Environ Toxicol 2017;32:1333–1342.
19. Scarparo RK, Dondoni L, Bottcher DE, Grecca FS, Figueiredo JA, Batista EL. Apical periodontium response to enamel matrix derivative as an intracanal medication in rat immature teeth with pulp necrosis: Radiographic and histologic findings. J Endod 2012;38:449–453.
20. Bonsignore LA, Anderson JR, Lee Z, Goldberg VM, Greenfield EM. Adherent lipopolysaccharide inhibits the osseointegration of orthopedic implants by impairing osteoblast differentiation. Bone 2013;52:93–101.
21. Colombo JS, Moore AN, Hartgerink JD, Souza RN. Scaffolds to control inflammation and facilitate dental pulp regeneration. J Endod 2014;40:S6–S12.
22. Gao LN, Cui YL, Wang QS, Wang SX. Amelioration of Danhong injection on the lipopolysaccharide-stimulated systemic acute inflammatory reaction *via* multi-target strategy. J Ethnopharmacol 2013;149:772–782.
23. de Assis GF, de Miranda TT, Magalhaes LMD, Dutra WO, Gollob KJ, Souza PEA, Horta MCR. Effects of bio-Oss and Cerasorb dental M on the expression of bone-remodeling mediators in human monocytes. J Biomed Mater Res B 2017;105:2066–2073.
24. Wei J, Xu M, Zhang X, Meng S, Wang Y, Zhou T, Ma Q, Han B, Wei Y, Deng X. Enhanced osteogenic behavior of ADSCs produced by deproteinized antler cancellous bone and evidence for involvement of ERK signaling pathway. Tissue Eng Part A 2015;21:1810–1821.
25. van Houdt CI, Tim CR, Crovace MC, Zanotto ED, Peitl O, Ulrich DJ, Jansen JA, Parizotto NA, Renno AC, van den Beucken JJ. Bone regeneration and gene expression in bone defects under healthy and osteoporotic bone conditions using two commercially available bone graft substitutes. Biomed Mater 2015;10:035003.
26. Mohammadi Z, Dummer PM. Properties and applications of calcium hydroxide in endodontics and dental traumatology. Int Endod J 2011;44:697–730.
27. Sobacchi C, Schulz A, Coxon FP, Villa A, Helfrich MH. Osteopetrosis: Genetics, treatment and new insights into osteoclast function. Nat Rev Endocrinol 2013;9:522–536.

28. Xiong Y, Yan K, Bentley WE, Deng H, Payne GF, Shi XW. Compartmentalized multilayer hydrogel formation using a stimulus-responsive self-assembling polysaccharide. ACS Appl Mater Inter 2014;6: 2948–2957.
29. Malafaya PB, Silva GA, Reis RL. Natural-origin polymers as carriers and scaffolds for biomolecules and cell delivery in tissue engineering applications. Adv Drug Deliver Rev 2007;59:207–233.
30. Renaud M, Farkasdi S, Pons C, Panayotov I, Collart-Dutilleul PY, Taillades H, Desoutter A, Bousquet P, Varga G, Cuisinier F, Yachouh J. A new rat model for translational research in bone regeneration. Tissue Eng Part C 2015;22:125–131.
31. Lohmann P, Willuweit A, Neffe AT, Geisler S, Gebauer TP, Beer S, Coenen HH, Fischer H, Hermanns-Sachweh B, Lendlein A, Shah NJ, Kiessling F, Langen KJ. Bone regeneration induced by a 3D architectured hydrogel in a rat critical-size calvarial defect. Biomaterials 2017;113:158–169.
32. Mordenfeld A, Hallman M, Johansson CB, Albrektsson T. Histological and histomorphometrical analyses of biopsies harvested 11 years after maxillary sinus floor augmentation with deproteinized bovine and autogenous bone. Clin Oral Implan Res 2010;21:961–970.
33. Park JC, Oh SY, Lee JS, Park SY, Choi EY, Cho KS, Kim CS. *In vivo* bone formation by human alveolar-bone-derived mesenchymal stem cells obtained during implant osteotomy using biphasic calcium phosphate ceramics or bio-Oss as carriers. J Biomed Mater Res B 2016;104:515–524.
34. van Houdt CI, Ulrich DJ, Jansen JA, van den Beucken JJ. The performance of CPC/PLGA and bio-Oss for bone regeneration in healthy and osteoporotic rats. J Biomed Mater Res B 2018;106:131–142.